Axolemmal and Septal Conduction in the Impedance of the Earthworm Medial Giant Nerve Fiber

Todd L. Krause,*‡ Harvey M. Fishman,‡ and George D. Bittner*

*Department of Zoology, Institute for Neuroscience, College of Pharmacy, University of Texas, Austin, Texas 78712, and ‡Department of Physiology & Biophysics, University of Texas, Medical Branch, Galveston, Texas 77555-0641 USA

ABSTRACT Ionic conduction in the axolemmal and septal membranes of the medial giant fiber (MGF) of the earthworm (EW) *Lumbricus terrestris* was assessed by impedance spectroscopy in the frequency range 2.5–1000 Hz. Impedance loci in the complex plane were described by two semi-circular arcs, one at a lower characteristic frequency (100 Hz) and the other at a higher frequency (500Hz). The lower frequency arc had a chord resistance of 53 kΩ and was not affected by membrane potential changes or ion channel blockers [tetrodotoxin (TTX), 3,4-diaminopyridine (3,4-DAP), 4-aminopyridine (4-AP), and tetraethylammonium (TEA)]. The higher frequency arc had a chord resistance of 274 kΩ at resting potential, was voltage-dependent, and was affected by the addition of TTX, 3,4-DAP, 4-AP, and TEA to the physiological EW salines. When all four blockers were added to the bathing solution, the impedance locus was described by two voltage-independent arcs. Considering the effects of these and other (i.e., Cd and Ni) ion channel blockers, we conclude that: 1) the higher frequency locus reflects conduction by voltage-sensitive ion channels in the axolemmal membrane, which contains at least four ion channels selective for sodium, calcium, and potassium (delayed rectifier and calcium-dependent), and 2) the lower frequency locus reflects voltage-insensitive channels in the septal membrane, which separates adjacent MGFs.

INTRODUCTION

The earthworm medial giant fiber (MGF) has been characterized morphologically as having septa that partition adjacent MGFs (Coggeshall, 1966). Several studies in MGFs have analyzed the conduction of gap junctions in the septal membrane (Brink and Barr, 1977; Brink et al., 1988; Brink and Fan, 1989) but have only alluded to the presence of sodium and potassium channels in the axolemmal membrane (Brink and Barr, 1977).

Studies in our laboratories have focused on understanding cellular responses of the MGF to injury, such as axonal sealing (Krause et al., 1994) and regeneration (Birse and Bittner, 1976; 1981; Lyckman and Bittner, 1992). We used impedance spectroscopy (rapid acquisition of complex impedance [$Z(jf)$] data and subsequent analysis and model fitting in the frequency domain (Fishman, 1992)) to quantify electrical changes in axolemmal integrity caused by injury and recovery from injury (Krause et al., 1994). In the course of these studies, we quantified the effect of specific ion-channel blockers on $Z(jf)$ and identified the types of voltage-sensitive axolemmal ion channels that dominate the impedance of the earthworm MGF. Further, we identified conduction in septa of MGFs from a voltage- and channel blocker-insensitive feature in $Z(jf)$.

Received for publication 30 March 1994 and in final form 27 May 1994.

Address reprint requests to Dr. Harvey Fishman, Department of Physiology & Biophysics, University of Texas, Medical Branch, Basic Science Building, Galveston, TX 77555-0641. Tel.: 409-772-1826; Fax: 409-772-3381; E-mail: fishman@beach.utmb.edu.

0006-3495/94/08/692/04 $2.00

MATERIALS AND METHODS

Preparation

The ventral nerve cord (VNC) of an adult earthworm contains one medial giant fiber (MGF) and two lateral giant fibers 15–20 cm in length. Each MGF is comprised of many (150–200) individual axons about 60–100 μm in diameter and 1–2 mm in length that are connected in series at their ends by low resistance gap junctions in membrane partitioning structures called "septa" (Bullock et al., 1965; Coggeshall, 1966; Brink and Barr, 1977). Each MGF is attached to its cell body by a long, thin (presumably high resistance) process (Mulloney, 1970; Gunther, 1975).

To obtain a VNC in vitro, we first anesthetized sexually mature earthworms in 0.2% (w/w) chloretone. Then, the VNC was dissected from the animal (see Krause et al., 1994) and pinned out in a Sylgard coated dish with a physiological earthworm saline (EWS) containing 40.1 mM NaCl, 10 mM Na_2SO_2, 25 mM Na-acetate, 0.5 K_2SO_4, 3.0 mM $CaCl_2$, 0.5 mM $MgCl_2$, 1.25 mM Tris, 1.4 mM HEPES, and 50–100 μM carbachol of pH 7.4 and 180 mOsm.

Impedance

The tips of two glass electrolyte-filled (3 M KCl) microelectrodes were placed intracellularly within 40 μm of each other for "driving-point" impedance measurements. Microelectrodes were placed between nerve roots where septa often exist in the MGF. Therefore, electrode-to-septum distance (0.5–1 mm) was less than one-third of the space constant of the preparation (2.5–3.5 mm). Current was applied through one electrode, and membrane voltage was recorded with the other electrode.

Impedance determinations were made by impedance spectroscopy (see Fishman, 1992). Briefly, a synthesized waveform composed of the sum of 400 sinusoids, from 2.5 to 1000Hz in increments of 2.5Hz, was applied repetitively to the preparation as a "small signal" current (10 nA) to elicit linear responses. The synthesized, periodic signal was synchronized with a sampled-data acquisition system and fast Fourier computation to preserve the phase relationships between response and driving sinusoids and to enable rapid collection of data (400 ms for a single impedance function of frequency). The measured driving current, $i(t)$, through the preparation was Fourier transformed to the frequency (f) domain to obtain the complex current, $I(jf)$, expressed in a data array and stored as *real and imaginary* [$j = (-1)^{-1/2}$] *parts* at each of the 400 discrete frequencies of the sinusoids

in the $i(t)$ waveform. The MGF voltage response, $v(t)$, to $i(t)$ was subsequently Fourier-transformed to give the complex voltage response, $V(jf)$, and stored as another data array of *real and imaginary values* at the same discrete frequencies at which determinations were made for $i(t)$. The complex impedance, $Z(jf)$, at each of the 400 discrete frequencies of the sinusoids that constituted $i(t)$ was then computed from the stored data arrays as the complex ratio $V(jf)/I(jf)$.

The complex impedance was expressed in rectangular form as

$$Z(jf) = R(f) + jX(f)$$

where the *real part*, $R(f)$, and *imaginary part*, $X(f)$, reflect the dissipative (resistive) and energy storage (capacitive) processes of the MGF conducting system, respectively. $Z(jf)$ determinations were plotted as $X(f)$ vs. $R(f)$ (complex plane plots) at each of the 400 frequencies of the sinusoidal components in $i(t)$. For each $Z(jf)$ determination, parameters in an impedance model (see next section) were varied systematically until a minimum mean square error between the *real and imaginary parts* of $Z(jf)$ and those of the model were obtained (see Fishman and Lipicky, 1991). The impedance locus of the model with these parameter values constituted the best fit to $Z(jf)$, which are represented by a solid line in each $Z(jf)$ plot.

In every MGF measured, three $Z(jf)$ determinations were made, one at the resting membrane potential (typically −70 mV) and one each at ±20 mV from the resting potential by applying a direct current beginning 400 ms before the data acquisition interval.

Impedance model

A series impedance model [$Z(jf) = Z_e(jf) + Z_s(jf) + Z_m(jf)$] was fitted to $Z(jf)$ data obtained from each MGF. In this simple model (Fig.1), Z_e is the ohmic access resistance (i.e., axoplasmic resistance and solution resistance to the bath ground electrode), R_e. $Z_s(jf)$ represents the voltage-independent impedance of the septum, and $Z_m(jf)$ represents the voltage- and time-dependent impedance of the axolemma (Cole, 1972). Values for each of the electrical elements in Fig. 1 were obtained from a fit of the series impedance model to $Z(jf)$ measured during a 20-mV hyperpolarization of the MGF from rest, a membrane potential at which voltage-dependent ion conduction should be negligible. $Z(jf)$ data were then obtained at resting potential and at a depolarization of 20 mV from rest. These data were fitted with the series impedance model holding the values for R_e and Z_s constant and equal to the values obtained in the hyperpolarized state, whereas Z_m was allowed to vary.

Pharmacological identification of ion channels

Known blockers of several common ion channel types (for potassium channel blockers see Castle et al., 1989; for calcium channel blockers, see Janis and Triggle, 1991) were added to the EWS to characterize their effect on $Z(jf)$ at resting membrane potential and at ±20 mV from resting potential. Tetrodotoxin [TTX; 1 mM] was used to block Na channels and 3,4 diaminopyridine [3,4,-DAP; 1 mM], 4-aminopyridine [4-AP; 1 mM] and tetraethylammonium [TEA; 20 mM] were used to block delayed rectifier potassium channels. 20 mM TEA was also used to block Ca-activated potassium channels.

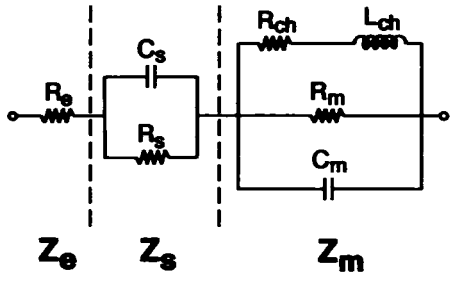

FIGURE 1 Series impedance model used to fit $Z(jf)$ data from the MGF. Z_e represents the ohmic access resistance (R_e). $Z_s(jf)$ represents the voltage-independent impedance of the septum, and $Z_m(jf)$ represents the voltage- and time-dependent impedance of the axolemma (Cole, 1972).

RESULTS

Pharmacological effects on $Z(jf)$ of the MGA

In the absence of any ion channel blockers, the sign of the *imaginary part* [$X(f)$] of $Z(jf)$ (Eq. 1) was positive from 2.5 to 25 Hz for a 20-mV depolarization from rest (see data points above abscissa for −50 mV locus in Fig. 2 *A*). An $X(f) > 0$ represents an inductive-like reactance caused by time- and voltage- dependent potassium and sodium conductances in the axolemmal membrane (Poussart et al., 1977), as first reported in the squid giant axon by Cole and Baker (1941). This inductive-like reactance remained

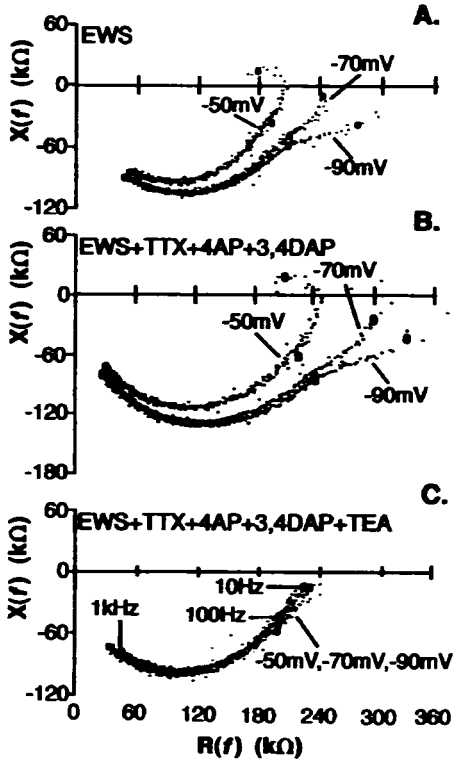

FIGURE 2 Effect of ion channel blockers on the MGF impedance determined at three transmembrane voltages in the same axon. $Z(jf) = R(f) + jX(f)$ plotted in the complex plane [$X(f)$ vs. $R(f)$]. Determinations were made at the 400 discrete frequencies in the range 2.5–1000Hz in 2.5Hz increments (see Materials and Methods). Frequency increases in a clockwise direction along all loci (See circled points labeled in *C*; the labels also apply to similar circled points in *A* and *B*). Data obtained at resting potential (−70 mV) and after voltage changes of ±20 mV from rest in the absence (*A*) or presence (*B*, *C*) of ion channel blockers added to EWS. (*A*) Voltage-sensitive $Z(jf)$ in EWS. Note, two separable loci. (*B*) Voltage-sensitive $Z(jf)$ in the presence of ion channel blockers TTX, 4-AP, and 3,4-DAP. Loci are larger because of blockage of Na^+ and K^+ channels. (*C*) Voltage-insensitive $Z(jf)$ in the presence of TTX, 4-AP, and 3,4-DAP *and* TEA. $Z(jf)$ loci are coincident at all potentials, indicating complete blockage of voltage-sensitive ion channels after addition of TEA to blockers in *B* (compare *B* and *C*).

(compare Fig. 2, *A* and *B*) when TTX, 4-AP, and 3,4-DAP were added to the EWS bathing the MGF to eliminate conduction in sodium and delayed rectifier potassium channels. When TEA was added to the EWS containing TTX, 4-AP, and 3,4-DAP to eliminate conduction in calcium-dependent potassium channels, the inductive-like reactance behavior disappeared, and the impedance locus was no longer voltage-sensitive, as indicated by the coincidence of the loci in Fig. 2 *C*.

To investigate further the presence of calcium-dependent potassium channels, we added 1 mM $CdCl_2$ and 1 mM $NiCl_2$ (to block calcium channels) to the EWS containing TTX, 4-AP, and 3,4-DAP. The effect of $CdCl_2$ and $NiCl_2$ on the impedance locus (data not shown) was similar to the effect of adding TEA. That is, $X(f)$ was no longer positive at low frequencies, and loci were coincident (as in Fig. 2 *C*). Because calcium channels are necessary to activate calcium-dependent potassium channels, these data are consistent with the hypothesis that the MGF contains calcium-dependent potassium channels.

Model of MGA complex impedance

The observation that $Z(jf)$ plots of the MGF displayed two separable loci, one at low frequencies and the other at higher frequencies, suggested that the MGF had two distinct impedances representing two membrane structures in series. Hence, we fitted a simple series-impedance electrical model (Fig. 1) to our $Z(jf)$ data from the MGF. Topologically, the passage of current from within an MGA should flow through the solution resistance between electrodes and sequentially through septal membrane and axolemmal membrane (corresponding to R_e, Z_s, and Z_m, respectively, in Fig. 1). Fig. 3 shows $Z(jf)$ data from the MGA, where the solid lines represent the best fit of our simple impedance model. Separate loci corresponding to the $Z_s(jf)$ and $Z_m(jf)$ portions of the model are plotted, respectively, as small semi-circular arcs and solid lines above the data points. Best fits of our model showed that values for the chord resistances, R_s in Z_s (53 ± 4.8 kΩ; $n = 4$) and R_m in Z_m (274 ± 29 kΩ; $n = 4$) are similar to values reported previously for R_s (Brink and Barr, 1977) and R_m (Dierolf and McDonald, 1969). These fits also yielded estimated values for C_s and C_m, which were 223 ± 122 nF ($n = 4$) and 1.3 ± 0.2 nF ($n = 4$), respectively. The apparently high estimate of C_s might be caused by a lack of sensitivity in determining the value of C_s from fits of the impedance function in the measured frequency range (2.5–1000Hz). Our best fit data also showed that the higher frequency arc was sensitive to ion channel blockers (especially TEA) and membrane potential, whereas the low frequency arc was not sensitive to ion channel blockers and membrane voltage.

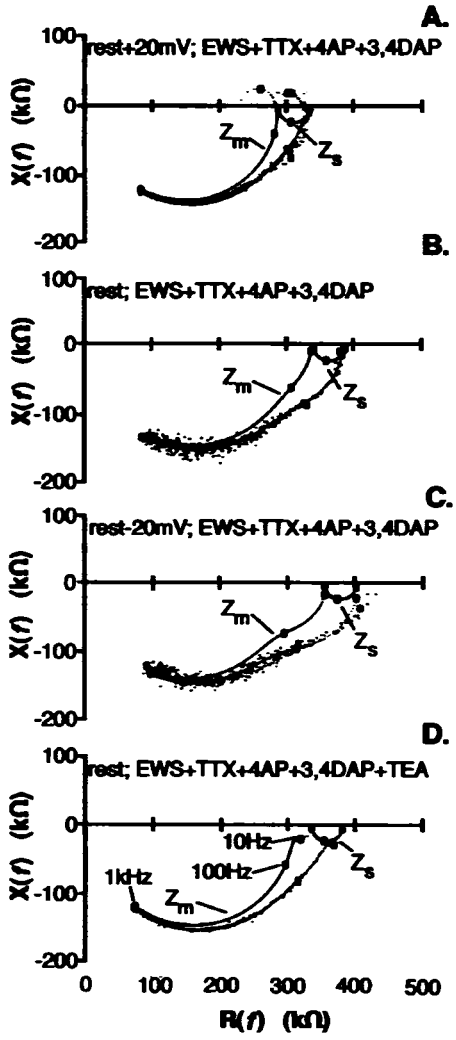

FIGURE 3 Best fits of MGF $Z(jf)$ according to the model shown in Fig. 1. $Z(jf)$ data (*points*) from an earthworm MGF bathed in normal saline (EWS) with TTX, 4-AP, 3,4-DAP (*A–C*) and TEA (*D*) at resting potential (*B, D*) and at ±20 mV from resting potential (*A, C*). Best fits of $Z(jf)$ data are shown as solid lines coincident with data points. The $Z_s(jf)$ and $Z_m(jf)$ portions of each $Z(jf)$ fit are shown separately. The frequency variable increases in a clockwise direction along all loci. Labeled frequencies of circled points in *D* also apply to similar points in *A, B,* and *C*. $Z_s(jf)$ was determined at hyperpolarized potential and assumed to be voltage and TEA-insensitive. $Z_m(jf)$ was assumed to be variable.

DISCUSSION

Previous studies have established that rapidly acquired complex impedance data can be used to characterize the conductance of various membrane ion channels in squid giant axon (Poussart et al., 1977; Fishman et al., 1983; Fishman and Lipicky, 1991; Fishman, 1992) and in somal membrane of molluscan neurons (Miyamoto and Fishman, 1986; Hayashi and Fishman, 1988). The main advantage of impedance measurements in excitable cells is that they do not require rapid, spatially uniform control of transmembrane voltage. Rather, zero frequency (dc) spatial control is sufficient to allow analysis and evaluation of complicated models. Consequently, membrane channels and structural properties can be analyzed simultaneously (Ebihara and Mathias, 1985).

The conducting properties of the MGF were evident in our impedance data without requiring a voltage-clamp system, which can be more difficult to implement because of the

impedance of septa in series with the axolemma and because of space clamp problems. Although a voltage clamp study of the axolemma of the MGF has not been reported, our data are consistent with previous studies of septa, which used a double voltage-clamp technique (Brink et al., 1988). Impedance measurements also provide a simpler way to study macroscopic properties of conduction by gap junction channels in the septal membrane of this preparation because they require two, rather than four, intracellular electrodes.

The $Z(jf)$ of squid giant axon is dominated at frequencies below 1000 Hz by ion channel conduction in a single structure (the axolemma). In the septate MGF of the earthworm, we have identified two distinct features in impedance loci that represent two separate conducting structures (the axolemma and septa), each with a different chord resistance and a different sensitivity to voltage and ion channel blockers.

Our findings are consistent with earlier reports that the resistance of the axolemma is much greater (270 kΩ vs. 50 kΩ) than that of a septum (Brink and Barr, 1977); axolemmal resistance is TEA-sensitive, whereas septal resistance is TEA-insensitive (Brink and Barr, 1977; Brink and Fan, 1989); and the septa do *not* have voltage-dependent ion channels (Brink and Barr, 1977; Verselis and Brink, 1984; Brink et al., 1988). Each of these qualities suggest that the higher frequency arc in our impedance loci [$Z_m(jf)$ in our model] is associated with the axolemma and that the low frequency arc [$Z_s(jf)$ in our model] is associated with septa. Because $Z_s(jf)$ was voltage-independent, we also ascribe the ion channels with the characteristics described above to the axolemmal membrane.

The ability to render the impedance of MGFs voltage-insensitive with ion channel blockers allowed us to assess changes in the dielectric properties of the membrane, which were of immediate interest for our studies characterizing the repair of membrane damage in the MGF (Krause et al., 1994). The effects of channel blockers upon impedance loci allowed us to identify tentatively several major ion channel types. In addition to the ion channels commonly found in axons (i.e., sodium and potassium), two less common channel types were also present (calcium and calcium-dependent potassium). Conduction in septa were also clearly evident in $Z(jf)$, which provides a simpler way to study conduction in gap junction channels that previously required a double voltage-clamp technique (Brink et al., 1988).

Supported in part by National Institutes of Health grant NS31256 (H. M. Fishman), Office of Naval Research grant N00014-90-J-1137 (H. M. Fishman), a Texas Advanced Technology Program grant (G. D. Bittner), and a National Institute on Alcohol Abuse and Alcoholism fellowship (T. L. Krause).

REFERENCES

Brink, P., and L. Barr. 1977. The resistance of the septum of the median giant axon of the earthworm. *J. Gen Physiol.* 69:517–536.

Brink, P. R., and S. F. Fan. 1989. Patch clamp recordings from membranes which contain gap junction channels. *Biophys. J.* 56:579–593.

Brink, P. R., S. W. Jaslove, R. T. Mathias, and G. Baldo. 1988. Voltage clamp studies of gap junctions. *In* Gap Junctions. E. L. Hertzberg and R. G. Johnson, editors. Alan R. Liss, Inc., New York. 321–334.

Bullock, T. H., and G. A. Horridge. 1965. Structure and Function in the Nervous Systems of Invertebrates. W. H. Freeman & Co., San Francisco.

Castle, N. A., D. G. Haylett, and D. H. Jenkinson. 1989. Toxins in the characterization of potassium channels. *TINS.* 12:59–65.

Cole, K. S. 1972. Membranes, Ions and Impulses: A Chapter of Classical Biophysics. University of California Press, Berkeley, CA.

Dierolf, B. M., and H. S. McDonald. 1969. Effects of temperature acclimation on electrical properties of earthworm giant axons. *Z. vergl. Physiologie.* 62:284–290.

Ebihara, L., and R. T. Mathias. 1985. Linear impedance studies of voltage-dependent conductances in tissue cultured chick heart cells. *Biophys. J.* 48:449–460.

Fishman, H. M. 1992. Assessment of conduction properties and thermal noise in cell membranes by admittance spectroscopy. *Bioelectromagnetics Suppl.* 1:87–100.

Fishman, H. M., H. R. Leuchtag, and L. E. Moore. 1983. Fluctuation and linear analysis of Na-current kinetics in squid axon. *Biophys. J.* 43: 293–307.

Fishman, H. M., and R. J. Lipicky. 1991. Determination of K^+-channel relaxation times in squid axon membrane by Hodgkin-Huxley and by direct linear analysis. *Biophys. Chem.* 39:177–190.

Gunther, J. 1975. Neuronal syncytia in the giant fibers of the earthworm. *J. Neurocytol.* 4:55–62.

Hayashi, H., and H. M. Fishman. 1988. Inward rectifier K^+-channel kinetics from analysis of the complex conductance of *Aplysia* neuronal membrane. *Biophys. J.* 53:747–757.

Janis, R. A., and D. J. Triggle. 1991. Drugs acting on calcium channels. *In* Calcium Channels: Their Functions, Regulation, and Clinical Relevance. L. Hurwitz, L. D. Partridge, and J. K. Leach, editors. CRC Press, Boca Raton, FL. Chapter 13.

Krause, T. L., H. M. Fishman, M. L. Ballinger, and G. D. Bittner. 1994. Extent and mechanism of sealing in transected giant axons of squid and earthworms. *J. Neurosci.* In press.

Krause, T. L., H. M. Fishman, and G. D. Bittner. 1992. Complex impedance of the medial giant fiber of earthworm. *Biophys. Soc. Am. Soc. Biochem. Mol. Biol. Abstr.* #2931.

Lyckman, A. W., S. M. Heidelbaugh, and G. D. Bittner. 1992. Analysis of neuritic outgrowth from severed giant axons in Lumbricus terrestris. *J. Comp. Neurol.* 317:1–13.

Miyamoto, S., and H. M. Fishman, 1986. Na conductance kinetics in the low-frequency impedance of isolated snail neurons. *IEEE Trans. Biomed. Eng. BME.* 33:644–653.

Mulloney, B. 1970. Structure of the giant fibers of earthworms. *Science.* 168:994–996.

Poussart, D., L. E. Moore, and H. M. Fishman. 1977. Ion movements and kinetics in squid axon. I. Complex admittance. *Ann. N.Y. Acad. Sci.* 303: 355–379.

Verselis, V., and P. Brink. 1984. Voltage clamp of the earthworm septum. *Biophys. J.* 45:147–150.